Defence Science Journal, Vol 49, No 5, October 1999, pp. 347-362
© 1999, DESIDOC

Albedo Variations and Surface Energy Balance in Different Snow-Ice Media in Antarctica

V.D. Mishra

Snow & Avalanche Study Establishment, Manali-175 103.

ABSTRACT

The present study is aimed at investigating the radiation budget in different snow-ice media (shelf ice, continental ice and natural snow) at three different elevated sites in the general area of Prince Astrid Coast of East Antarctica. Measurements of the dependence of albedo in different snow and ice media on solar elevation angle, cloud cover, liquid water content, grain size, etc. can be interpreted in terms of single and multiple scattering radiative transfer theory. Detailed albedo measurements were carried out during summer and winter in different snow and ice media in 1997-98 at different selected sites at Antarctica. The average albedo values were found to be high (90 per cent) in snow medium, moderate (83 per cent) in shelf ice and very low (50 per cent) in continental ice medium. The albedo was found to be a function of cloud amount, increasing with the amount and thickness. In white-out condition during blizzards, high albedo (average 83 per cent) was found as compared to clear sky day (76 per cent) and after blizzard (average 78 per cent). It showed dependence on the type and age of snow also. New snowfall over old snow displayed higher values (90 per cent) than older snow (70 per cent) and decreased with the age of snow from 13-16 per cent. Natural melt-water in snowpack increases from 1-10 per cent, resulting in albedo decay from 7-10 per cent. As the minimum solar elevation angle in Antarctica goes to 3°, strong qualitative analyses have been made of the dependence of albedo on the solar elevation angle. Albedo values showed diurnal hysteresis and morning values were found to be higher than evening values at the same angle of elevation. The dependence was slight for solar elevations during day time when $\theta >\approx 12–15°$, but became larger with low angles when $\theta = 3–12°$. Solar insolations were also calculated for different months in order to calculate short wave radiation absorbed by snow and ice media. Insolations in different months at different selected sites lie in the ranges 10-540 ln/day (August-October), 350-911 ln/day (November-December) and 190-755 ln/day (January-February). Net energy balance was calculted using model and was found to be negative most of the time.

NOMENCLATURE

ΔQ Net change in energy storage of a snow-ice surface (energy balance) (ln/day)

Q_{rs} Net short wave radiation received by the snow-ice surface (ln/day)

Q_{rl} Net long wave radiation received by the snow-ice surface (ln/day)

Q_{in} Downward long wave radiation from the atmosphere to snow-ice surface (ln/day)

Q_l Latent heat flux due to evaporation or condensation/sublimation (ln/day)

Q_s Sensible heat flux at snow/ice – air interface by conduction (ln/day)

Q_g Heat exchange at snow-ground interface (ln/day)

Revised 23 August 1999

Q_m	Advected heat flow (ln/day)
T_a	Air temperature 2m above snow-ice surface (K)
T_s	Snow surface temperature (K)
a	Fractional albedo
R_o	Energy received at the top of atmosphere (ln/day)
R	Energy received at snow-ice surface on a clear day (ln/day)
Q_i	Energy received on the snow surface (ln/day)
Z	Height of clouds (low and thick– 2000 m, medium–5000 m. and high– 8000 m)
N	Cloud amount in fraction of sky covered (octa)
A_c	Integrated albedo for cloudy sky condition (in per cent)
A_o	Integrated albedo for clear sky condition (in per cent)
K	Cloud type (0.76 for low clouds, 0.52 for medium clouds and 0.26 for high clouds)
Z_a	Height of albedometre (m)
Z_o	Roughness height of the surface (0.005 m for smooth surface and 0.0007 m for snow on grass)
K_w	Eddy transfer coefficient for vapour
k	Von Karman's constant (0.4)
σ	Stefan - Boltzmann constant (1.36 × 10^{-12} ln K^{-4} s^{-1} or 5.67 W m^2 K^{-4})
ρ_a	Standard density of air (1.1 x 10^{-3} g/cm^3)
e_a	Saturated vapour pressure at air temperature T_a (Pa)
e_s	Saturated vapour pressure at snow surface temperature T_s (Pa)
V_a	Wind velocity at the height of observation (m/s)
g	Gravitational acceleration (9.81 m/s^2)
$(R_I)_B$	Bulk Richardson number
$(R_I)_{cr}$	Critical Richardson number (0.2-0.5)
C_p	Specific heat of ice at constant pressure (0.24 cal/g/K)
L	Latent heat of sublimation (677 cal/g)
ϵ	Dielectric constant of snow-ice medium
ξ	Emissivity of the medium
ρ	Density of snow-ice (g/cm^3)
P	Atmospheric pressure (101300 Pa)
W	Free liquid water content in snow (per cent by volume)

1. INTRODUCTION

The interaction of electromagnetic radiation with a natural snowcover is of considerable scientific importance. The remote sensing community requires thorough understanding of the optical properties of snow in order to correctly interpret the imagery of snowcovered regions and to distinguish between snowpack and cloud covers. Radiant energy transfer is important in the thermodynamics and metamorphosis of snowpack and is, therefore, of interest to scientists studying mechanical and hydrological properties of the snowpack. Therefore, the establishment of relationships between the optical properties of snow and the frequently measured snowpack quantities, such as liquid water content, density, surface temperature, etc. would be of considerable utility.

To understand how ablation on a glacier may change if climate changes, one needs to know the albedo and components of the surface energy balance. It is generally accepted that at least on mid-latitude valley glaciers, the most important processes delivering melt energy in summer are absorption of solar radiation and turbulent exchange of sensible heat. On most glaciers, solar radiation typically provides 75 per cent of the melt energy, although on the lower parts of maritime glaciers this may be closer to 50 per cent.

In recent years, glacier mass balance models have been developed based on calculation of all energy transfers between the atmosphere and the glacier surface[1-3]. Radiative and turbulent energy fluxes are calculated from climatological data. The surface balance can be prescribed as calculated using an energy balance model[4,5]. The energy balance model is an attractive tool for simulating the surface balance, since the physical processes on the surface can be described fairly explicitly in the model. Such studies were usually performed over a short period in one medium and at a single location. Inspite of the energy balance work done so far, there is still a need for glacio-meteorological radiation data for a long period and at larger areas.

It is, however, not easy to obtain such data continuously around the year due to ablation zones and other problems related to tremendous weather changes in Antarctica. An attempt was made to record the radiation and snow-met data as and when possible. Furthermore, for budgetary and logistic reasons, it is not feasible to have a permanently manned station at different sites on a glacier tongue.

In this study, field work was carried out at three different sites. One site was located on the snow surface (snowpack in Antarctica is formed due to natural snowfall , snow drift and blizzards) in front of the permanent Indian base station *Maitri* (70°46'S, 11°45'E). *Maitri* is located on Schirmacher oasis to the west of Dakshin Gangotri with the Wohlthat mountain chain lying towards the south[6]. The second site was chosen on the Polar ice cap (blue ice or continental ice) about 7 km from *Maitri* and the third site for scientific observatory was on the shelf ice at Dakshin Gangotri (70°05'S, 12°E). An analysis of the solar radiation measurements from August 97–February 98 in different snow-ice media has been presented. Quantification of dependence of albedo on different physical parameters, and the net energy budget has been done hourly and daily by incorporating a simple energy balance model.

2. EXPERIMENTAL DETAILS

Due to the importance of albedo, radiative fluxes in the energy balance model , priority was given to accurate radiation measurements. At all the selected sites in Antarctica, global radiation and reflected global radiation were measured using two precision pyranometers, one facing upwards and the other downwards. These instruments have a nominal sensitivity of 7-8 $\mu V/W/m^2$. They have a flint glass double dome with excellent transmission characteristics for solar radiation in the wavelength range 0.3-3 μm. The instrument was kept at a height of 1.5 m on flat snow-ice surface in order to minimise the cosine error in the measurements due to slope. Glacio-met data were obtained using meteorological instruments. Snow surface temperature, a very important parameter, was measured using a dial type sensor thermometer having measuring range −50 °C to + 50 °C with an accuracy of ± 0.5 °C. Free liquid water content in the snowpack was measured using dielectric moisturemeter having a capacitive sensor plate. The sensor was first calibrated in air and the dielectric constant was then measured after inserting the plate in the snowpack. Liquid water content in the snowpack was measured using following relationship:

$$\epsilon' = 1+(1.92x\rho)+0.44\rho^2+0.187W+0.0046W^2 \qquad (1)$$

3. ENERGY BALANCE APPROACH

3.1 Physical Processes

Snowcover gains and loses energy by various processes. It gains heat from insolation, long wave radiation from the atmosphere and clouds, advection of warm air, latent heat released by condensation or sublimation of moisture on the snow surface, sensible heat transfer (if air is warmer than the snow surface), and conduction from the ground underneath. On the other hand, snowpack loses heat to its environment by long wave radiation, evaporation or sublimation from the snowcover, and sensible heat, (if air is colder than snow). Heat transfer also occurs within the snowpack due to penetration of solar radiation, conduction and change of state like solid-liquid, solid-vapour and vice versa.

3.2 Energy Balance Model

The energy received at the snow surface is considered to be utilised in (i) satisfying the cold contents of the top layer, (ii) absorption in the top layer, (iii) conduction at the surface, conduction and diffusion through the underlying layer, and (iv) producing melt.

Net change in energy storage of a glacier or snowcover[7-9] is expressed as

$$\Delta Q = Q_{rs} + Q_{rl} + Q_l + Q_s + Q_g + Q_m \tag{2}$$

The heat exchange at snow-ground interface is very little and the advected heat also does not contribute to the energy exchange at Antarctica. Net change in energy storage at the snow/ice–air interface is

$$\Delta Q = Q_{rs} + Q_{rl} + Q_l + Q_s \tag{3}$$

3.2.1 *Short Wave Radiation*

Short wave radiations reaching the snow surface are reflected, transmitted and absorbed by snow. The amount of energy absorbed and reflected depends on the physical properties of snow both at and beneath the surface. Albedo is the most important physical property of snow which controls the amount of radiation absorbed. The expression for the net short wave radiation can be:

$$Q_{rs} = Q_i(1-a) \tag{4}$$

Direct solar radiation reaching earth's surface can be measured using meteorological observations. The portion of the insolation that actually reaches the earth's surface depends upon the transparency of the atmosphere and the optical air mass through which it must pass. Some of the incident solar radiation is reflected, some scattered, and some absorbed by the atmosphere. In the absence of clouds, these amounts are relatively small and quite constant barring unusual atmospheric conditions, such as dust storms. The variations that occur are mainly due to variations in the amount of water vapour and dust in the air. The smaller the optical air mass, the greater is the transmission for any given condition of the atmosphere. Atmospheric transmission coefficient is defined as the ratio of the insolation received at the earth's surface through a cloudless sky to the insolation received at the outer limit of the earth's atmosphere. The atmospheric coefficient varies from about 80 per cent at the time of the winter solstice to about 85 per cent at the time of the summer solstice. Experiments conducted by US Army Corps of Engrs showed that radiation incident on the surface on a clear day[10] is:

$$Q_i = R[1-(0.82-0.000073Z)N] \tag{5}$$

$$\begin{aligned} R &= 0.8\ R_o \text{ (winter period)} \\ &= 0.85 R_o \text{ (summer period)} \end{aligned} \tag{6}$$

3.2.2 *Long Wave Radiation*

The radiative property of snow in the range 3-40 μm implies radiative exchanges strictly confined to the snow/ice surface. For long wave radiation, snow behaves nearly like a perfect black body, i.e., it absorbs all such radiation falling upon it and emits radiation according to Stefan–Boltzmann law[11]. Long waves are received by the snow surface as back radiation from all levels of the atmosphere. Back radiation depends on the distribution of moisture, pollutants, cloudiness and temperature in the entire atmosphere. However, it has been suggested that the downward long wave radiation from the atmosphere can be estimated from surface air temperature and vapour pressure alone[9] as

$$Q_{in} = \sigma T_a^4 (A + B\sqrt{e_a}) \tag{7}$$

where

$$\xi = (A + B\sqrt{e_a}), \quad A = 0.47 \text{ and } B = 0.061$$

$$e_a = 8 - 18\,(h\text{Pa})$$

On a cloud-free day, the net long wave radiation input to the snowcover is:

$$Q_{nl} = \sigma(\xi T_a^4 - T_s^4) \tag{8}$$

Clouds, being formed from liquid water droplets, absorb more long wave radiation than water vapour and hence act as a perfect black body. Under cloudy conditions, the net long wave radiation input to the snowcover is given by the following expression:

$$Q_{rl} = \text{Long wave (in)} - \text{Long wave (out)}$$
$$= \sigma\,(\xi T_a^4 - T_s^4)\,(1 - KN) \qquad (9)$$

3.2.3 *Latent & Sensible Heat Flux*

The turbulent exchange processes occurring within 2-3 m above the snow surface govern both latent and sensible heat fluxes.

Latent heat flux is expressed as

$$Q_l = 0.622\,K_w \rho_a L[e_a - e_s]\,V_a / P \qquad (10)$$

$$K_w = K_N\,[1 - (R_I)_B / (R_I)_{cr}]^2 \qquad (11)$$

$$K_N = k^2 / [\ln(Z_a / Z_o)]^2 \qquad (12)$$

$$(R_I)_B = (2gZ_a / V_a^2)[T_a - T_s]/[T_a + T_s] \qquad (13)$$

$$e_a = \tfrac{1}{2}[6.1078 \exp\{17.2693882(T_a - 273.16) / T_a - 35.80)\}] \qquad (14)$$

Sensible heat flux is expressed as

$$Q_s = \rho_a C_p K_w [T_a - T_s] V_a \qquad (15)$$

4. RESULTS & DISCUSSION

4.1 Average Albedo Variation in Different Media

The daily average albedo on snow, continental ice and shelf ice is shown in Figs 1, 2 and 3, respectively. The higher average albedo value has been found in snow medium (average 90 per cent) as compared to shelf ice (average 83 per cent)) and continental ice (average 50 per cent). Snow is a mixture of air, water and snow particles but continental ice consists of only pure ice particles closely packed and having hexagonal structures. The ice layers present within the Antarctic shelf ice and continental ice partially contribute to reflected radiation. A major part of the incident radiation falling over the ice sheet is transmitted down, resulting in low albedo values.

The density for all the three media was found to be in the range 0.25-0.38 g/cc for snow, 0.35-0.48 g/cc for shelf ice and 0.85-0.89 g/cc for continental ice. There have been many reports[12] of albedo decreasing as density increases. The observed dependence of albedo on density might actually be a dependence on grain size, since large density is normally attributed to larger grain size. Due to the presence of larger grains on the surface, there is a

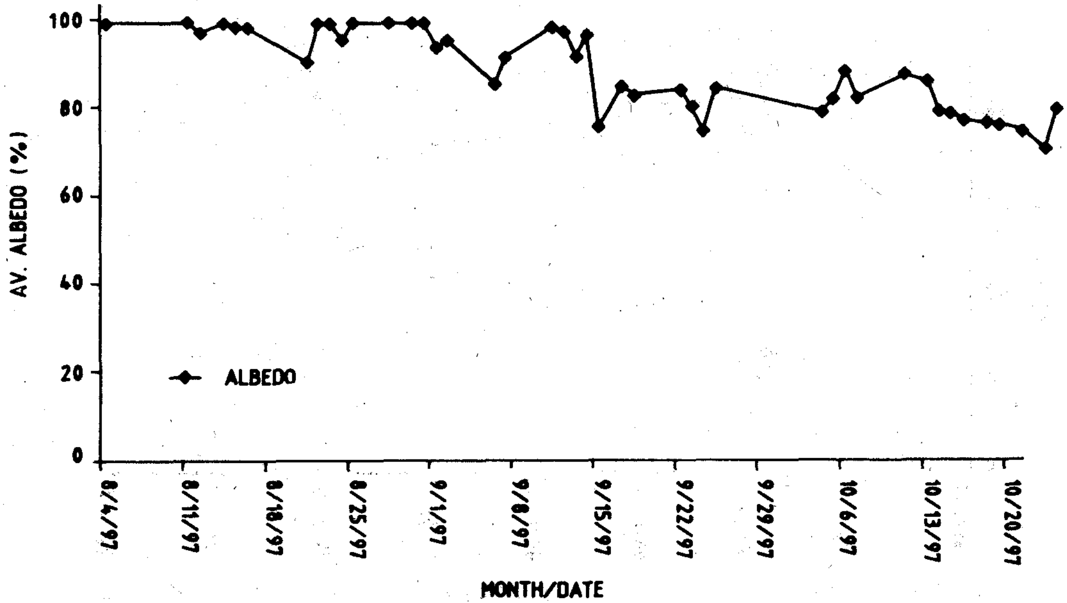

Figure 1. Daily albedo variation on the snow surface

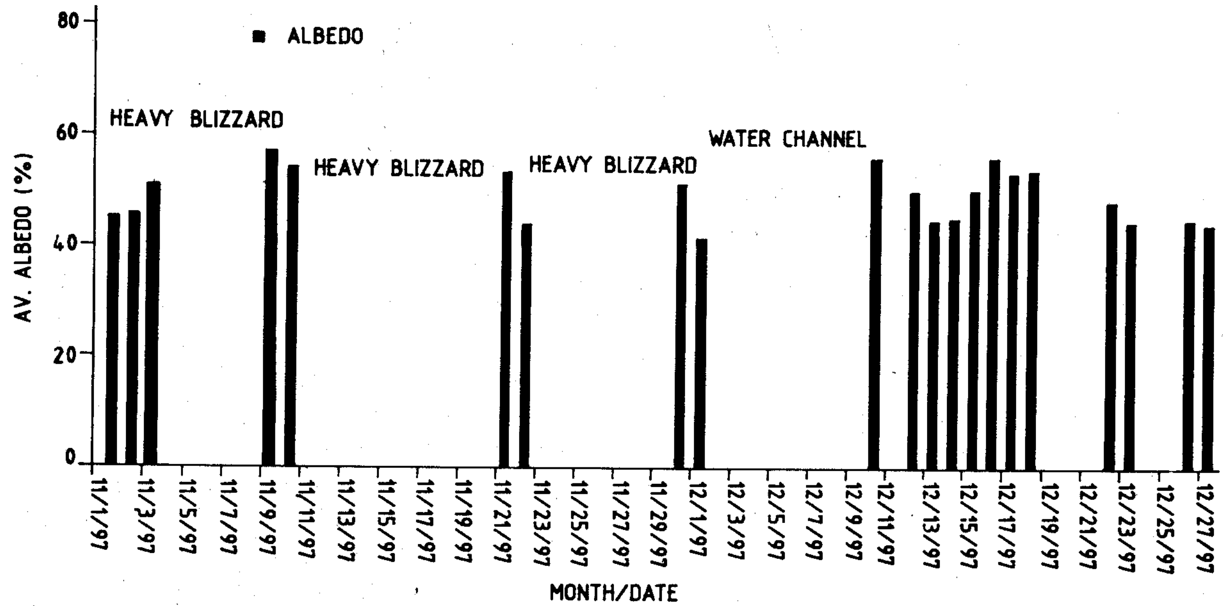

Figure 2. Albedo values on the continental ice surface

chance that the ray may be scattered or bent when it crosses an air-ice interface. It has a chance of being absorbed only while it is passing through the ice. Increase in grain size also causes an increase in the path length that must be traversed through the ice between scattering opportunities.

4.2 Albedo Variation with Cloud Amount

The daily average albedo and the average cloud amount were calculated by simple arithmetic means to know their mutual variation. The albedo values are found to increase with increase in the cloud amount as shown in Fig. 4. To know the dependence of albedo on the thickness of clouds, observations were taken during clear sky day, at the time of blizzard, and after blizzard (Fig. 5). The average albedo was found to be higher (83 per cent) during white-out condition in blizzard when cloud thickness is very high as compared to clear sky day (76 per cent) and after blizzard, (78 per cent). It can

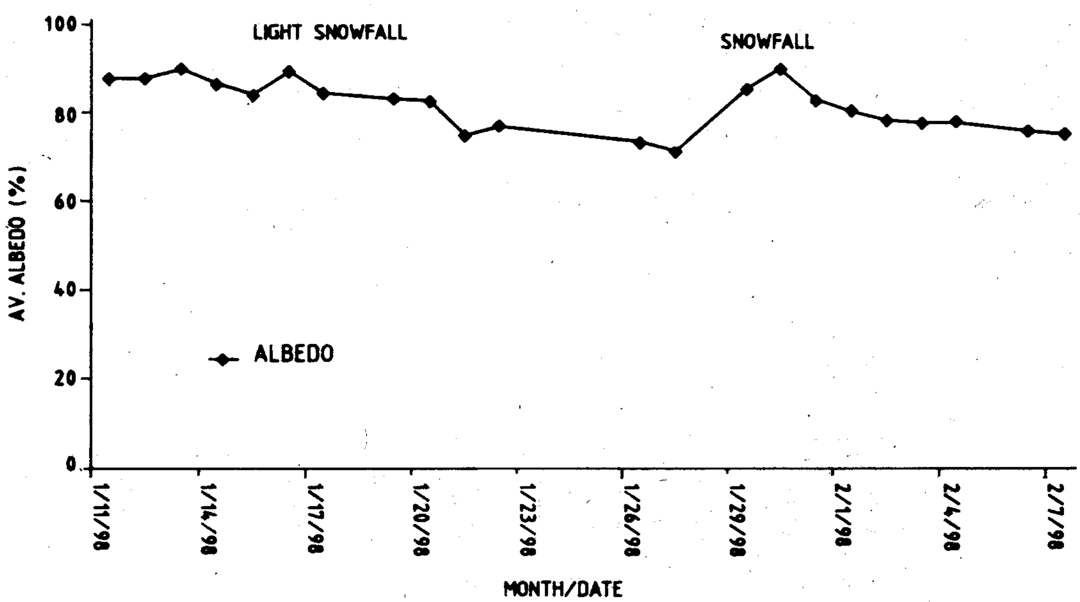

Figure 3. Albedo variation on the shelf ice surface

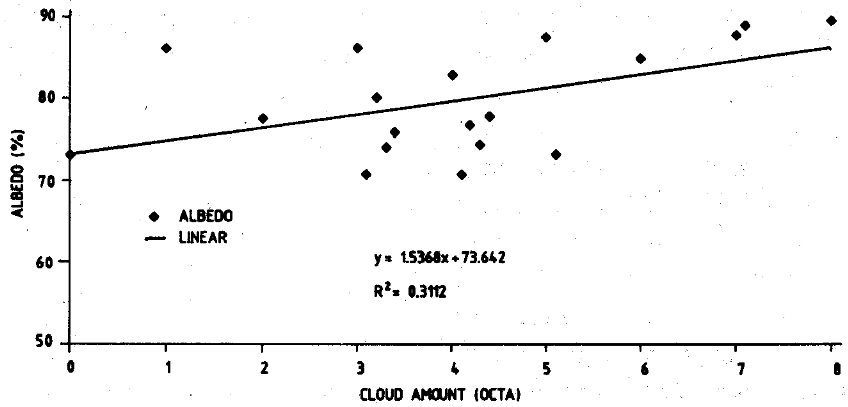

Figure 4. Albedo variation with cloud amount

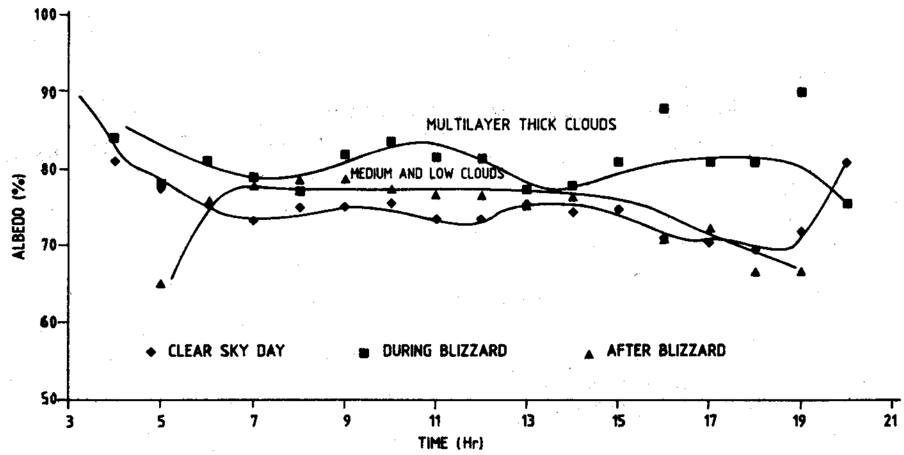

Figure 5. Albedo variation under different cloud conditions

be inferred that albedo is a function of both cloud amount and cloud thickness and increases with increasing cloud amount and thickness. The increase in albedo can be attributed to the fact that clouds absorb a larger part of infrared than visible radiation. Thus, a relatively larger portion of visible radiation reaches the surface under cloudy conditions. Because the visible snow albedo is high (> 0.90) compared to the near-infrared albedo (≈ 0.50), an increase in surface albedo is to be expected during overcast weather[12,13]. The average albedo values are found to show an excellent correlation with cloud amount. The average albedo value increases from 74 to 85 per cent as the cloud amount increases from 0 to 8 octa. Using the data set of the above measurements, an empirical relationship has been formulated, which can be used for evaluating the percentage increase in albedo for cloudy sky condition if the clear sky albedo value is known. The expression is:

$$A_c = 1.5368*(N) + A_o \qquad (16)$$

4.3 Albedo Decay with Age of Snowpack

A very peculiar characteristic of snow is the decay of its albedo value with age of the snowpack. For fresh branched grain snow, albedo has exceptionally high values, ranging from 85–90 per cent. However, as the age of the snow surface increases, a typical decrease in albedo has been reported by US Army Corps of Engineers[14] and Pertzold[15]. None of the earlier studies has satisfactorily provided any explanation for this variation and the physical processes involved in it. The mathematical relationship proposed by Petzold to predict the albedo decay process was found to be only 12 per cent accurate. Detailed investigations on the decay process under natural conditions have been carried out. Albedo decay with age of snowpack on the shelf ice is shown in Figs 6(a) and (b) for 16–23 January 1998 and 30 January–7 February 1998, respectively. Observed and predicted values are shown. Predicted (1) are values of albedo when cloud consideration is not taken into account after a snowfall event. Predicted (2) are values of albedo when clouds are also considered, if there is cloudy weather after a snowfall event. Predicted (1) values are calculated using model proposed for the non-melting period during winter[16].

$$A(n) = \text{Base albedo} - 0.0473\, n^{1/2} \tag{17}$$

where

$A(n)$ = Albedo on n^{th} day after fresh snowfall event

n = Days after snowfall event

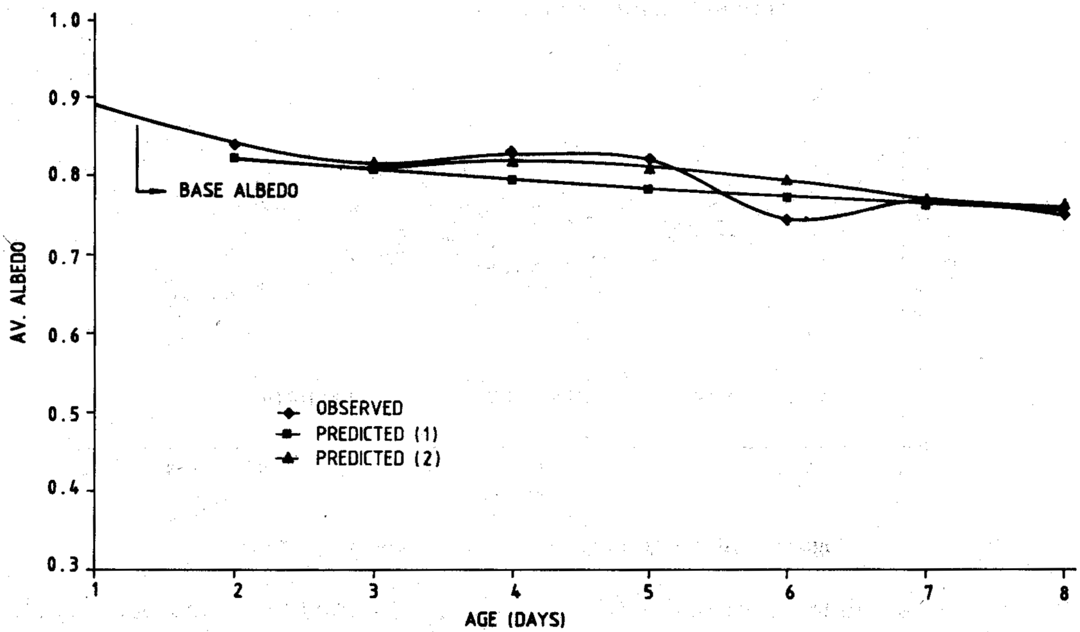

Figure 6(a). Albedo decay with age of snowpack

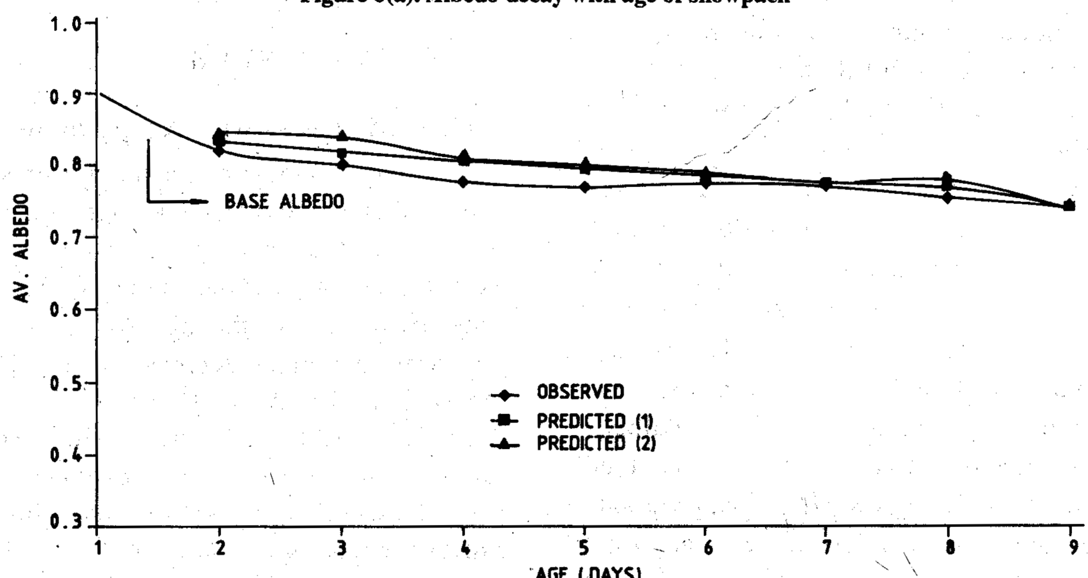

Figure 6(b). Albedo decay with age of snowpack

In the present study, the base albedo is taken as albedo on the first day after a fresh snowfall event. Predicted (2) albedo values are calculated using the following empirical relationship:

$$A(n) = A(1) - [0.0473 n^{1/2} (1 - K N)] \tag{18}$$

where

$A(1)$ = Albedo on the first day after snowfall event.

It can be observed that there is a good correlation between the observed and the predicted albedo values, as shown in Figs 6(a) and (b). Investigations during the present study indicate a sharp decline in albedo for the first 4-5 days after snowfall event followed by a gradual decline. Mainly three processes have been found to govern the rate of decay, namely, (i) the rate and type of snow metamorphism, (ii) increase in snow grain size and melt-water amount, and (iii) accumulation of impurities over snow surface . After the fresh snowfall event, the snow grains present on the surface of snowpack are generally faceted and have a highly branched structure like stellar grains. The branches of these grains act as reflecting mirrors for the incident radiation causing glitter in the snow field. As the temperature rises, the vapour pressure difference over the convex and concave surfaces of these grains leads to mass transfer from convex to concave surfaces and hence destruction of the sharp edges and rounding of the snow grains. The rate of loss of the branches is rapid and the entire grain takes a roundish shape within 1-3 days, depending on the prevailing temperatures. This results in a very sharp decline in albedo values for the first 4-5 days after fresh snowfall event. On an average, a decay of 3-4 per cent per day has been observed for the first few days after the snowfall event, as shown in Figs 6(a) and (b).

After the loss of sharp edges, the later stages of metamorphic process of snow grains increases the snow grain radii. Subsequently, increase in grain radius takes over the control of decrease in albedo values. The process of grain growth under equi-temperature metamorphism is quite slow, resulting in slower decay rates (1-2 per cent). As the snow ages, addition of impurities like pollen grains, soot, dust, etc. leads to decrease in albedo values in the visible spectrum. Production of melt water on the snow surface increases the rate of grain growth and reduces the albedo in the near-infrared spectrum. The combined effect of these parameters influences albedo decay with the age of snowpack.

4.4 Albedo Variation with Melt-Water

The values of real part of refractive index of ice and water are different from each other in the near-infrared spectral range and water has stronger absorption bands as compared to snow/ice as reported by Irvines[17], *et al.* Presence of melt-water even in small quantities reduces reflectance of snow surface significantly.

Under natural conditions when the snow melts, the condensation nuclei get released from the ice matrix and are deposited on snow surface, whereas the melt-water percolates down the surface. The cumulative addition of such impurities makes the snow surface dirty, thereby reducing reflectance in the visible spectrum. This highlights the reason why even after refreezing of the melt-water during evening hours when temperatures are relatively low, the albedo does not return to its original higher value. Another important factor that contributes to reduction in albedo values is increase in effective snow grain size due to melt-water deposition over small grains, because refractive index contrast between water and ice is very small[12]. The increase in snow grain size plays a more prominent role as compared to the surface impurities.

Experimental investigations in the laboratory also lead to the observation that as the amount of free water on snow surface increases, there is a decrease in reflectance. However, an interesting phenomenon has been observed, when the amount of free water over the snow surface is increased continuously. After the saturation limit of the capillary retentivity is reached, the water trapped between grains over the snow surface percolates down suddenly. This results in reduction of free water and decrease in effective grain radii, leading

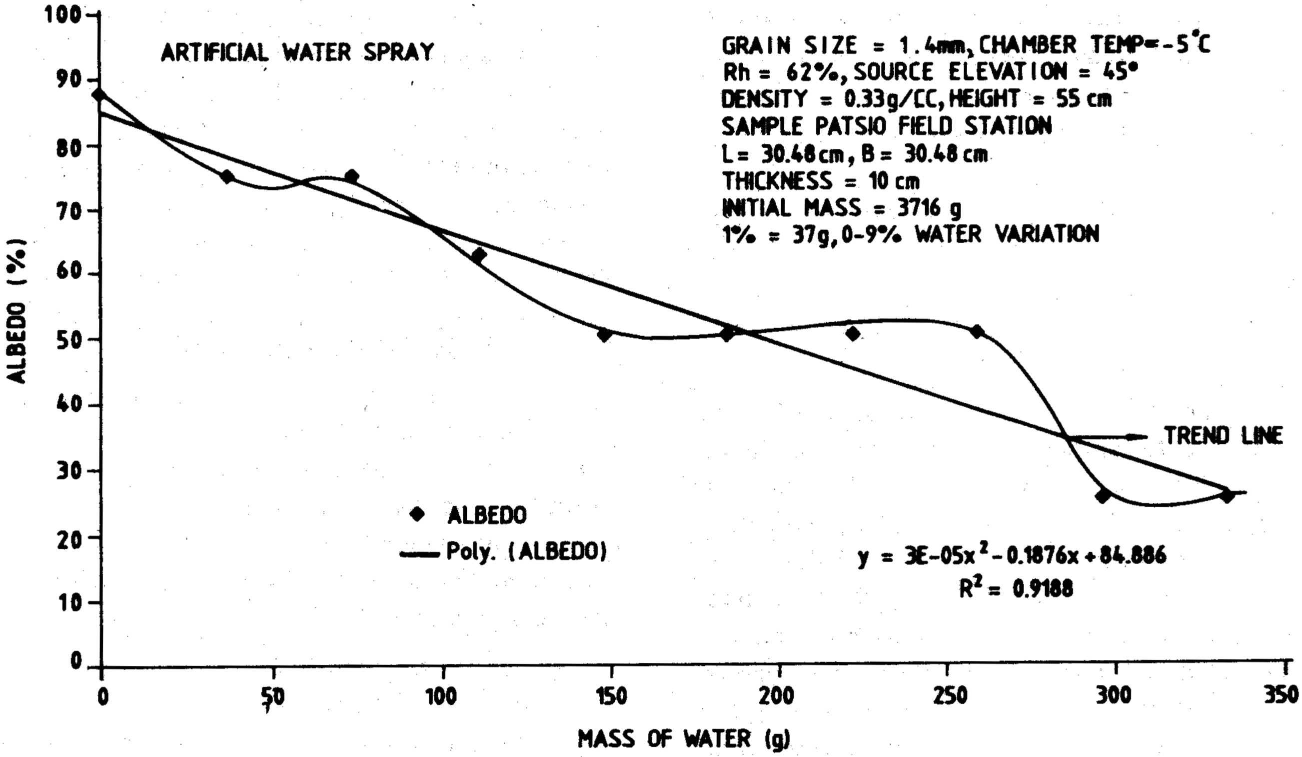

Figure 7(a). Albedo variation with artificial melt-water

to a sudden increase in albedo values, as shown in Fig.7(a). On further addition of water, again the pore space between snow grains starts accumulating water and reflectance starts decreasing with increase in the amount of water.

Figs. 7(b) and (c) highlight decrease in integrated albedo with increase in melt-water amount over snow and the antarctic ice shelf. These figures indicate that integrated albedo values decrease by 7-8 per cent with increase in water

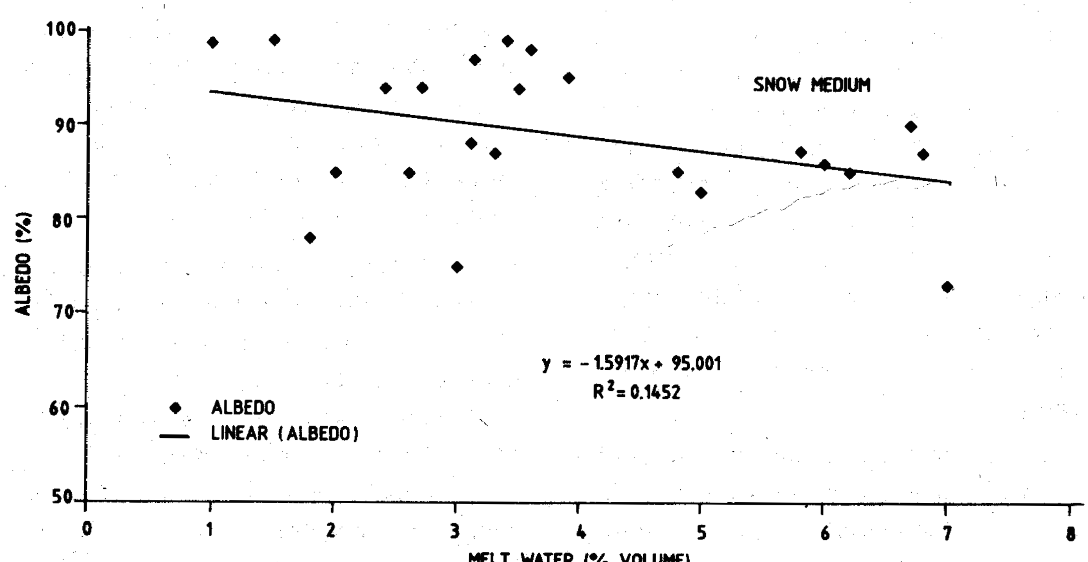

Figure 7(b). Albedo variation with natural melt-water in snowpack

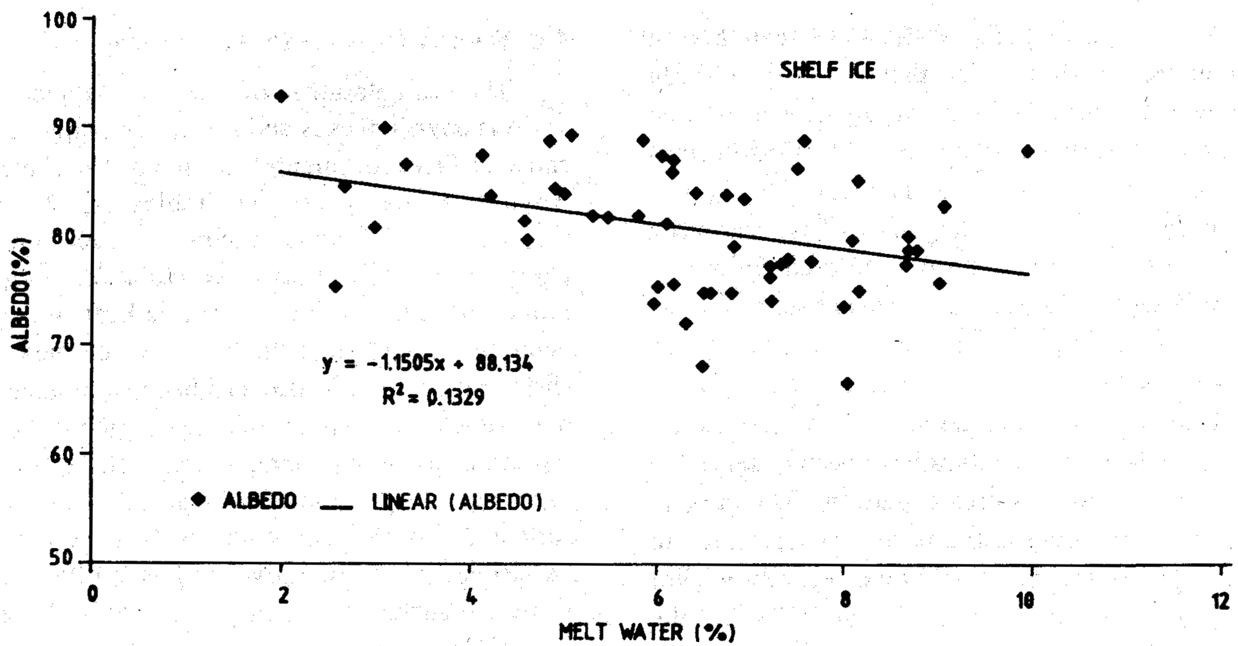

Figure 7(c). Albedo variation with natural melt-water in shelf ice

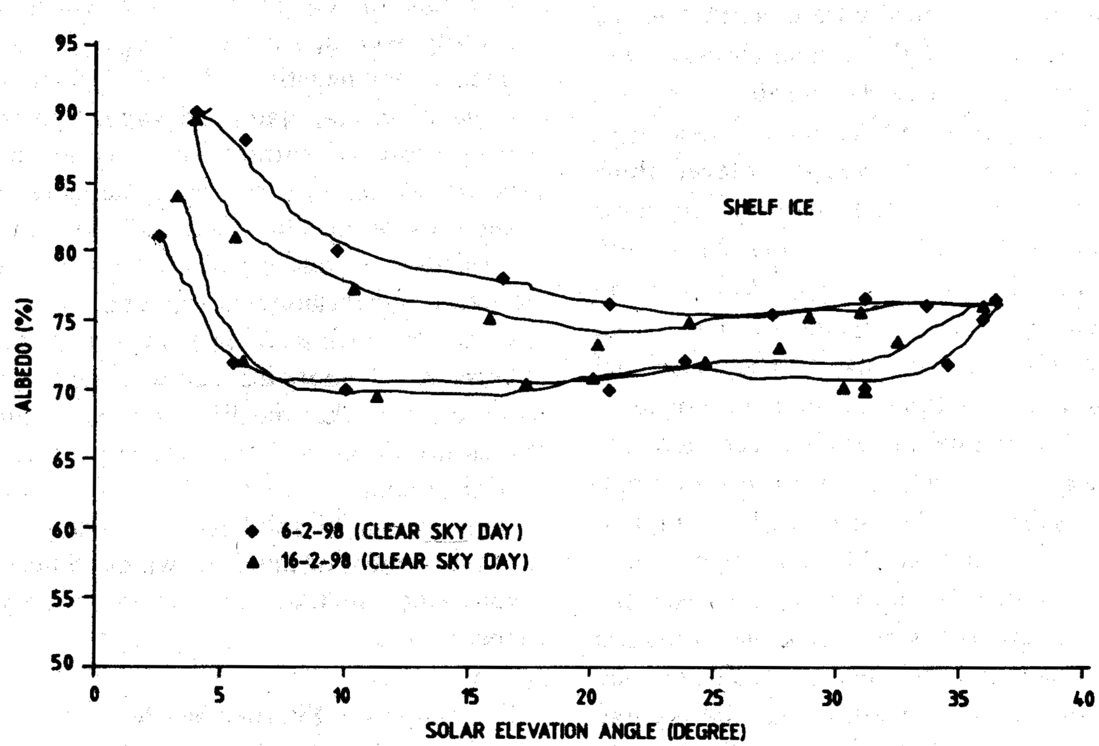

Figure 8. Diurnal hysteresis of snow albedo

amount by 1-10 per cent. The scatter in data values can be attributed to variation in many other parameters influencing snow albedo.

4.5 Albedo Variation with Solar Elevation

Decrease in albedo values has been observed on clear sky days with increase in solar elevation from 3–12° (approx.) (Fig.8). It can be seen that for solar elevation above 12°, there is only a slight dependence of the albedo. It was also observed that when sun is near the horizon ($\theta \approx 3°$), albedo values are found to be very high. The reason is that a photon on an average undergoes its first scattering event closer to the surface if it entered snow at a grazing[12] angle. If the scattering event sends it in an upward direction, its chance of escaping the snowpack without being absorbed is greater than it would be if it were scattered from deeper in the snowpack. The albedo values have been observed to follow a diurnal hysteresis pattern. The albedo value in the morning is found to be higher than in the afternoon for identical solar elevation. For example, on 16 Feburary 1998 at 0700 hr, the ambient temperature was 265.5 K and the surface albedo value was 0.74 and on the same day at 1600 hr, the ambient temperature was 269.5 K and albedo value 0.70, although the solar elevation was 20°. The hysteresis may be attributed to the formation of thin, weak coating of hoar-frost layer. It was observed that the thin hoar-frost layer which has a shining surface and is a feather type crystal is generally formed during clear sky and is due to very low temperature below ice point in early morning and late evening. These phenomena have been reported by other authors also[18]. The individual values of snow albedo derived from hourly incident and reflected radiation measured over snow-ice surface result in a periodicity of 10 hr. (approx.). The variation should be attributed to diurnal deposition and evaporation of the hoar-frost coating from the snow surface. As the temperature rises, the thin layer of hoar-frost is removed due to intense incident solar radiation. In other words, one can say that it remains in wet or melting state during day time and is again formed in the late evening or early morning due to very low temperature. The hysteresis is due solely to the value of reflected radiation being less in the afternoon than in the morning for identical solar elevation. This indicates that the effect is due to some change in the snow surface properties.

4.6 Energy Balance in Antarctica

The calculations of energy balance using various energy fluxes and insolation estimates over snow surface, continental ice and on the shelf ice in Antarctica are given in Tables 1, 2 and 3, respectively. Various incoming and outgoing energy fluxes like short wave radiation, long wave radiation, latent heat and sensible heat fluxes have been calculated for different snow-ice media. The short wave radiation flux has been calculated using the albedo of snowpack and global incident radiation as input parameters. The short wave radiation flux is positive and is absorbed and reflected by the snow-ice surface. Long wave radiation flux is negative and is emitted by the snow-ice surface according to Stefan's Boltzmann law. The latent heat flux is the result of melting and freezing of snow and the sensible heat flux arises as a result of temperature differences and wind activity over the snow-ice surface. It can have both positive and negative values. When latent heat flux is positive, e.g., saturated vapour pressure of air over snow-ice surface is more as compared to saturated vapour pressure of the snow-ice surface and snow surface temperature $T_s = 0°$, water vapour condenses as liquid water on the melting glacier surface. When saturated vapour pressure of air over snow-ice surface is less than saturated vapour pressure of snow-ice surface, sublimation takes place. Also, when the difference of saturated vapour pressure of air and snow-ice is positive and snow surface temperature $T_s < 0°$, there is condensation from vapour to solid ice. The energy balance is negative most of the time, which indicates that the snow-ice surface is losing energy to the atmosphere.

5. Scope for Further Work

Albedo is one of the important parameters which play a significant role for snow melt run off and climate modelling. The albedo data along with other physical parameters proposed for energy balance model can be incorporated in mass balance models also. A correlation can be developed between energy balance and mass balance. It

Table 1. Variation energy fluxes and insolation on the snow surface

Date	Insolation (ln/day)	Q_{rs} (ln/day)	Q_{rl} (ln/day)	Q_l (ln/day)	Q_s (ln/day)	ΔQ (ln/day)
4.8.97	11.940	4.905	-124.680	-29.600	34.150	-115.240
11.8.97	23.880	2.190	-136.590	-60.900	57.900	-137.300
12.8.97	31.840	13.430	-140.960	61.240	27.650	-161.200
14.8.97	26.865	0.500	-156.860	-59.400	-15.280	-231.020
15.8.97	5.275	0.290	-93.740	-21.310	-15.630	-130.350
16.8.97	10.746	0.380	-143.300	-44.530	-17.730	-205.190
21.8.97	9.950	18.050	-88.400	-51.150	-61.820	-59.670
22.8.97	53.730	0.370	-173.560	-68.000	-59.900	-301.080
23.8.97	61.690	1.300	-151.190	-15.390	-4.650	-169.910
24.8.97	79.600	10.150	-131.700	-38.220	33.410	-126.350
25.8.97	59.700	4.160	-138.320	-26.000	-20.170	-180.410
28.8.97	81.590	4.730	-168.310	-76.240	-180.280	-420.120
30.8.97	99.500	8.350	-171.500	-32.800	-50.500	-246.420
31.8.97	97.510	4.000	-142.200	-16.320	-14.820	-169.350
1.9.97	113.430	21.500	-166.720	-20.690	-48.500	-214.500
2.9.97	117.410	22.900	-119.900	-11.850	-24.800	-84.000
7.9.97	91.540	25.000	-148.490	-24.710	-27.160	-201.300
8.9.97	115.420	24.630	-102.400	-50.500	150.700	22.500
11.9.97	177.110	7.070	-143.200	-14.850	-19.970	-170.770
12.9.97	185.080	14.600	-151.910	-43.200	-15.600	-196.120
13.9.97	145.270	24.450	-144.750	-36.500	-60.170	-216.920
14.9.97	187.060	17.960	-163.900	-19.530	-30.500	-195.920
15.9.97	29.850	39.420	-49.700	-11.210	-45.620	24.120
17.9.97	216.910	42.000	-117.000	-45.380	4.750	-115.600
18.9.97	91.540	28.660	-63.050	-0.800	0.930	-34.260
22.9.97	226.860	34.000	-68.000	-4.500	3.100	-40.000
23.9.97	214.920	49.990	-99.000	-9.990	-5.400	-64.500
24.9.97	304.470	89.900	-134.500	-46.800	31.800	-59.400
25.9.97	57.000	49.200	-117.400	73.000	65.000	-76.200
4.10.97	312.360	75.600	-165.500	-35.700	-16.500	-142.000
5.10.97	354.220	73.600	-164.000	-42.800	-45.900	-179.000
6.10.97	244.770	27.400	-67.940	-41.400	-11.800	-120.900
7.10.97	338.300	66.300	-163.200	-43.800	-26.000	-166.800
11.10.97	147.260	29.600	-119.600	-131.900	58.300	-163.510
13.10.97	378.100	47.300	-125.220	-44.200	-26.000	-97.600
14.10.97	453.720	85.900	-164.800	-36.900	-12.900	-128.800
15.10.97	457.700	80.500	-158.500	-42.310	1.700	-118.500
16.10.97	465.660	88.800	-180.500	-66.400	-54.000	-212.200
18.10.97	491.530	91.900	-171.600	-24.300	-11.800	-115.700
19.10.97	491.530	99.200	-196.900	-63.950	-97.900	-259.500
21.10.97	501.570	66.700	-145.210	-52.500	-29.200	-160.140
23.10.97	541.280	95.300	-142.000	-35.000	0.660	-81.200
24.10.97	435.810	83.000	-144.600	-44.800	8.700	-115.000

Table 2. Various energy fluxes and insolation on the continental ice surface

Date	Insolation (ln/day)	Q_{rs} (ln/day)	Q_{rl} (ln/day)	Q_l (ln/day)	Q_s (ln/day)	ΔQ (ln/day)
1.11.97	634.810	199.700	-184.000	-363.230	-388.200	-73.620
2.11.97	591.030	139.180	-143.900	-172.300	- 87.160	-264.130
3.11.97	477.600	118.400	-143.000	-267.800	-191.500	-483.900
9.11.97	687.600	128.400	-132.800	-51.700	63.410	7.400
10.11.97	710.430	147.900	-139.200	-84.970	87.950	11.600
21.11.97	753.220	205.700	-166.800	-75.000	16.900	-19.200
22.11.97	755.040	185.250	-169.300	-182.410	13.280	-153.100
30.11.97	837.800	159.700	-165.100	-192.900	27.610	-170.800
1.12.97	567.150	178.200	-133.300	-189.900	106.900	-37.900
10.12.97	795.000	169.370	-150.700	-31.240	2.520	-10.050
12.12.97	742.310	130.870	-116.900	-130.200	11.900	-104.300
13.12.97	636.900	200.600	-174.600	-81.100	11.600	-43.600
14.12.97	841.900	198.600	-167.500	-93.980	13.700	-49.300
15.12.97	516.400	139.200	-135.900	-91.400	16.900	-71.200
16.12.97	739.200	150.700	-159.000	-78.000	20.400	-70.000
17.12.97	757.300	170.500	-168.000	-88.900	17.900	-68.800
18.12.97	354.300	151.600	-135.000	-115.900	52.000	-47.200
22.12.97	701.000	204.000	-141.700	-37.400	33.500	58.600
23.12.97	897.600	225.800	-141.000	-85.400	81.400	80.710
26.12.97	733.400	206.300	-136.700	-82.000	76.300	63.900
27.12.97	911.500	219.900	-137.400	-54.400	55.800	83.900

requires some basic information on snow–ice depth, snowfall events, melt-water amount, cloud condition, transmissivity, emissivity, etc. The available models can be improved if large areas can be covered with continuous radiation data for longer periods. To ensure consistency, the observations can be made by automatic weather stations at different locations and also through remote sensing. To develop a strong correlation of albedo with different physical parameters, remote sensing also requires continuous monitoring of ground truth data at different sites. With large radiation data for long periods, one can approach for climate modelling.

6. CONCLUSIONS

Results are presented from measurements carried out during August 1997–February 1998 in different snow-ice medium, in Queen Maudland, in Antarctica. Glacio-meteorological and albedo measurements were carried out in the immediate vicinity of a blue ice area, on shelf ice as well as on natural snow. The surface energy balance was evaluated using a simple model and the measured meteorological parameters. The differences in the surface energy balance between snow and ice can be attributed mainly to the differences in albedo, surface roughness, thermal conductivity and short wave radiation extinction coefficient. The long wave radiation flux, latent heat flux and sensible heat flux are mainly responsible for energy exchange at the snow-ice-air interface. A good qualitative analysis of albedo dependence on melt-water and cloud amount is obtained. A correlation of albedo with cloud amount and melt-water is a very important parameter for use in energy balance model.The dependence of albedo on the age of snowpack gives an idea about the metamorphic activity in the snowpack. Diurnal

Table 3. Various energy fluxes and insolation on the shelf ice surface

Date	Insolation (ln/day)	Q_{rs} (ln/day)	Q_{rl} (ln/day)	Q_l (ln/day)	Q_s (ln/day)	ΔQ (ln/day)
11.1.98	716.940	29.600	-109.800	-116.500	-7.000	-203.800
12.1.98	296.600	10.900	-42.200	-114.900	-8.400	-173.000
13.1.98	350.800	10.910	-42.900	-130.400	29.700	-132.800
14.1.98	629.330	43.900	-164.000	-103.500	-12.000	-211.700
15.1.98	755.200	58.700	-178.100	-108.000	4.700	-222.900
16.1.98	422.900	30.800	-128.200	-89.800	7.300	-179.900
17.1.98	735.700	48.400	-174.800	-97.800	8.200	209.900
20.1.98	501.600	42.800	-143.000	-81.800	-3.600	-185.700
21.1.98	329.500	61.300	-131.200	-57.310	9.400	-117.800
26.1.98	363.700	56.700	-143.000	-104.300	32.800	-157.900
27.1.98	217.000	53.300	-119.600	-50.300	12.900	-103.700
29.1.98	346.900	15.000	-46.500	87.600	0.880	-118.000
30.1.98	234.700	10.500	-43.200	-64.800	8.000	-89.600
31.1.98	659.700	65.000	-144.300	-71.600	10.400	-140.600
5.2.98	420.000	205.000	-155.400	-63.440	38.400	24.600
6.2.98	651.300	209.000	-189.200	-81.600	-3.200	-65.000
7.2.98	629.600	163.500	-158.600	-94.300	-1.960	-91.400
9.2.98	510.000	180.900	-177.200	-70.600	-5.600	72.600
15.2.98	500.000	210.700	-168.500	-86.000	31.800	-12.000
16.2.98	640.000	299.000	-265.500	-204.500	15.700	-156.000
17.2.98	610.000	70.000	-139.000	-150.000	20.000	-199.000
18.2.98	540.000	150.000	-70.000	-179.000	15.000	-84.000
19.2.98	190.000	180.000	-60.000	-150.000	-10.000	-40.000
22.2.98	575.000	170.000	-200.000	-124.000	5.000	-149.000
23.2.98	410.000	140.000	-100.000	-170.000	-170.000	-299.000

hysteresis of snow albedo indicates that the effect of hoar-frost will be dependent on the strength of solar radiation, snow-ice surface and ambient temperature.

ACKNOWLEDGEMENT

The author thanks all member of the XVI Indian Antarctic Expedition for their help and support during the expedition. He is grateful to Maj Gen S.S. Sharma, KC, VSM, Director, SASE and Shri D.N. Sethi, Dy Director, for their constant encouragement, scientific discussions and presentation and also for granting permission to publish this work.

REFERENCES

1. Gruell, W. & Oerlemans, J. Sensitivity studies with a mass-balance model including temperature profile calculations inside the glacier. *Z. Gletscherkd Glazialgeol.*, 1986, **22**(2), 101-24.

2. Oerlemans, J. A model for the surface balance of ice masses, Part 1, Alpine glaciers. *Z. Gletscherkd Glazialgeol.*, 1991-1992, **27-28**, 63-83.

3. Oerlemans, J. & Fotuin, J.P.F. Sensitivity of glaciers and small ice caps to green house-warming. *Science.*, 1992, **258** (5079), 115-17.

4. Anderson, A. Eric. A point energy and mass-balance model of a snowcover. NOAA Technical Report No. NWS-19, 1976.

5. Oerlemans, J. The mass-balance of the Greenland ice sheet: Sensitivity to climate change as revealed by energy-balance modelling. *Holocene*, 1991, **1**(1), 40-49.

6. Bhattacharya, B.B. Schirmacher oasis: Environment, history and the Indian Station *Maitri*. Scientific Report of Fourth Indian Expedition. Department of Ocean Development, New Delhi, India, 1987. Technical Publication-4. pp.171-86.

7. Bintanja, R. & Vanden Broeke, M.R. Local climate, circulation and surface energy balance of an antarctic blue ice area. *Annals of Glaciology*, 1994, **20**, 160-68.

8. Brun, E. *et al.* An Energy and mass-balance model for snowcover for operational avalanche forecasting. *Journal of Glaciology*, 1989, **121** (35), 333-40.

9. Upadhyay, D.S. Cold climate Hydrometeorology. New Age International (P) Ltd., India.

10. U.S. Army Corps of Engineers. Snow hydrology. North Pacific Division, Portland, OR, 1956. 437 p.

11. Gubler, H. Energy and mass-balance, Swiss Federal Institute for Snow and Avalanche Research (SFISAR), Davos, Switzerland. pp. 51-65.

12. Warren, S.J. Optical properties of snow. *Rev. Geophys. Space Phys*., 1982, **20**(1), 67.

13. Male, D. H. & Graanger, R. J. Snow surface energy exchange. *Water Resour. Res*.,1981, **17**(3), 609.

14. U.S. Army Corps of Engineers. Snow hydrology, summary of papers on snow investigations. North Pacific Division,1955.

15. Petzold, D.E. An estimation technique for snow albedo. Climatology Bulletin, 1977, **21**..

16. Heather, E. & Heinz, G. Stefan. Albedo models for snow and ice on fresh water lake. *Cold Regions Sci. Technol.*, 1999, **29**, 31-48.

17. Irvines ,W.M. & Pollack, J.B. Infrared optical properties of water and ice spheres. *Icarus*, 1968, **8**.

18. Mcguffie, K. & Henderson-Sellers, A. The diurnal hysteresis of snow albedo. *Journal of Glaciology*, 1985, **108** (31), 188-89.

Contributor

Dr VD Mishra obtained his PhD (Condensed Matter Physics) from the Indian Institute of Technology, New Delhi, in 1996. He joined DRDO in 1996 and is presently working at the Snow & Avalanche Study Establishment (SASE), Manali, as Scientist C. He participated as a winter member for sixteen months in the XVI Indian Antarctic Expedition. He has published two research papers in international journals. He is currently working on radiation studies of snow in the Himalayan region.